A VISCOUS FLOW CALCULATION OF THE STERN FLOW

Shin-Hyoung Kang*, Keon-Je Oh and Toshio Kobayashi*****

(Received November 15, 1990)

Two computer codes have been developed to solve the Reynolds averaged Navier-Stokes equations; namely the fully elliptic method and the partially parabolic method. These are applied to simulate flows over the stern of the SSPA model as a bench mark, and also a multi-purpose ship with a barge type stern. The numerically generated body-fitted coordinate system is used to manage the complex geometry of the ship hull. A standard form of the k-ϵ turbulence model is adopted for modelling of the Reynolds stresses. Simulated results by both methods are nearly identical and the partially parabolic method can save about a half of the memory storage and 20% of CPU time in comparison with the fully elliptic method. The capability of programs is confirmed by sucessfully simulating pressures, skin frictions and mean velocities over sterns of the two models. Simulated nominal wake fractions show good accordance with wake measurements and the viscous resistance is accurate enough for the hull form design.

Key Words: Stern Flow, Navier-Stokes Equation, Partially Parabolic Navier-Stokes Equation, Boundary-Fitted Coordinate, k-ϵ Model

1. INTRODUCTION

The importance of the viscous flow simulations around the ship hull has received wide acknowledgement in the light of the hull-form design. Prediction of the viscous resistance is useful in the stage of the bare hull-form design. Ship forms of good resistance and propulsion performance cannot be developed without considering the propulsion effciency as well as the form factor. Such design and developement process can be enhanced, if numerical method can estimate form factors, nominal and effective wakes on the propeller plane, and thrust deduction factors. These design parameters can not be reasonably obtained without complex three-dimensional turbulent flow simulations over the ship stern and in the wake.

Viscous flows over the ship hull have been calculated by the three-dimensional boundary layer theory. If free surface effects are excluded, experiments and calculations indicate that first-order boundary layer equations are adequate for the flow over a large part of the ship length(Larsson, 1981). Experimental information pertaining to the evolution of the flow over the stern as well as in the near wake has been reviewed by Patel(1982). Much research works have been done for thick boundary layers over the stern in the past, but they have not provided a designer with valuable information.

The partially parabolic type of the Navier-Stokes equations instead of the fully elliptic Navier-Stokes(NS) equations have been recently employed to simulate the complex viscous flow over the stern in consideration of physical phenomena that there is usually no region of flow reversal in the direction of ship motion. These equations can be used to describe flows between the thin boundary layer upstream and the wake far downstream from the ship. The partially parabolic Navier-Stokes(PPNS) equations have been first employed to calculate flows and heat transfer in the straight square duct by Pratap and Spalding(1976). Abdelmeguid et al.(1979) was the first to apply the PPNS equation to the stern flow. Further research results were presented by Muraoka(1980, 1982), and by Janson and Larsson(1985), Raven and Hoekstra(1985), Tzabiras(1985). Chen and Patel(1985) adopted the finite analytic numerical scheme and produced reasonably accurate results for an axisymmetric body of revolution and three-dimensional mathematical models. We also have developed a computer program STERN/PPNS based on the partially parabolic method and the program has proved to be reasonably accurate in describing the pressure and velocity distributions around the stern(Kang et al., 1978a, 1988, 1989)

In the present study, for the extension of this method to treat the flow reversal over the hull and for the comparison between the partially parabolic and fully elliptic numerical procedures, calculation with the NS equations is carried out. Computer code STERN/NS for the fully elliptic NS equations is developed and the results by the NS and PPNS equations are investigated by the comparison between each others. Also, the possibility of the programs for design purposes is tested by estimating the viscous resistance and nominal wakes without propeller in the propeller plane. In a hull form design, these parameters are obtained by the emperical law or simple flat plate correlations. Therefore, if these parameters can be accurately predicted, we can provide pratically important data for the ship design.

*Department of Mechanical Engineering, Seoul National University, Shinrim-dong, Kwanak-ku, Seoul 151-742, Korea
**Department of Mechanical Engineering, Kyungnam University, 449 Wolyoung-dong, Masan 630-701, Korea
***Professor, Institute of Industrial Science, University of Tokyo, Roppongi 7-22-1, Minato-ku, Tokgo 106, Japan

2. GOVERNING EQUATIONS AND BOUNDARY CONDITIONS

2.1 Governing Equations

Geometry of the ship hull is described in the cylindrical coordinate system (x, r, θ) as shown in Fig. 1. Governing equations for the incompressible, steady, and turbulent flow are given by the continuity and Reynolds averaged Navier-Stokes equation. Reynolds stresses are modelled by using k-ϵ turbulence model In k-ϵ model the eddy viscosity is given by turbulence kinetic energy k and dissipation rate ϵ which are obtained from their transport equations. In the cylindrical coordinate, above governing equations can be written in general form as follows;

$$\frac{\partial}{\partial x}(U\phi)+\frac{1}{r}\frac{\partial}{\partial r}(rV\phi)+\frac{1}{r}\frac{\partial}{\partial\theta}(W\phi)=\frac{\partial}{\partial x}\left(\Gamma_\phi\frac{\partial\phi}{\partial x}\right)+\frac{1}{r}\frac{\partial}{\partial r}\left(r\Gamma_\phi\frac{\partial\phi}{\partial r}\right)+\frac{1}{r}\frac{\partial}{\partial\theta}\left(\Gamma_\phi\frac{\partial\phi}{\partial\theta}\right)+S_\phi \tag{1}$$

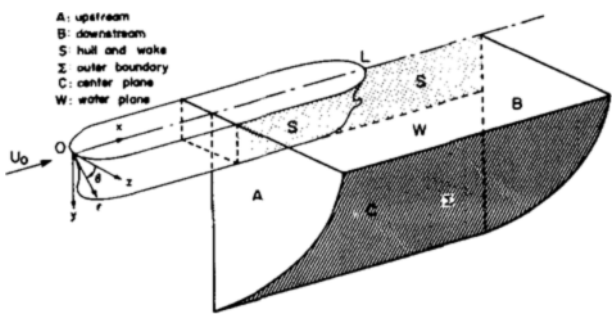

Fig. 1 Physical domain and coordinate system

Table 1 ϕ, Γ_ϕ and S_ϕ for the governing equation.

ϕ	Γ_ϕ	S_ϕ
1	0	0
U	ν_e	$-\frac{1}{\rho}\frac{\partial p}{\partial x}+\frac{\partial}{\partial x}\left(\nu_t\frac{\partial U}{\partial x}\right)+\frac{1}{r}\frac{\partial}{\partial r}\left(r\nu_t\frac{\partial V}{\partial x}\right)+\frac{1}{r}\frac{\partial}{\partial\theta}\left(\nu_t\frac{\partial W}{\partial x}\right)$
V	ν_e	$-\frac{1}{\rho}\frac{\partial p}{\partial r}+\frac{\partial}{\partial x}\left(\nu_t\frac{\partial U}{\partial r}\right)+\frac{1}{r}\frac{\partial}{\partial r}\left(r\nu_t\frac{\partial V}{\partial r}\right)+\frac{1}{r}\frac{\partial}{\partial\theta}\left(\nu_t\frac{\partial W}{\partial r}\right)+\frac{W^2}{r}-\frac{1}{r^2}\frac{\partial}{\partial\theta}(\nu_t W)-\frac{2\nu_e}{r^2}\frac{\partial W}{\partial\theta}-\nu_e\frac{V}{r^2}-\nu_t\frac{V}{r^2}$
W	ν_e	$-\frac{1}{\rho r}\frac{\partial p}{\partial\theta}+\frac{\partial}{\partial x}\left(\frac{\nu_t}{r}\frac{\partial U}{\partial\theta}\right)+\frac{1}{r}\frac{\partial}{\partial r}\left(\nu_t\frac{\partial V}{\partial\theta}\right)+\frac{1}{r}\frac{\partial}{\partial\theta}\left(\frac{\nu_t}{r}\frac{\partial W}{\partial\theta}\right)-\frac{1}{r}\frac{\partial}{\partial r}(\nu_t W)+\frac{2}{r}\frac{\partial}{\partial\theta}\left(\frac{\nu_t}{r}V\right)-\nu_e\frac{W}{r^2}-\frac{VW}{r^2}+\frac{\nu_t}{r}\frac{\partial W}{\partial r}+\frac{\nu_e}{r^2}\frac{\partial V}{\partial\theta}+\frac{\nu}{r^2}\frac{\partial V}{\partial\theta}$
k	$\frac{\nu_e}{\sigma_k}$	$G-C_D\epsilon$
ϵ	$\frac{\nu_e}{\sigma_\epsilon}$	$\frac{\epsilon}{k}(C_1G-C_2\epsilon)$

note; $G=\nu_t\left\{2\left[\left(\frac{\partial U}{\partial x}\right)^2+\left(\frac{\partial V}{\partial r}\right)^2+\left(\frac{1}{r}\frac{\partial W}{\partial\theta}+\frac{V}{r}\right)^2\right]+\left(\frac{\partial U}{\partial r}+\frac{\partial V}{\partial x}\right)^2+\left(\frac{1}{r}\frac{\partial U}{\partial\theta}+\frac{\partial W}{\partial x}\right)^2+\left(\frac{1}{r}\frac{\partial V}{\partial\theta}+\frac{\partial W}{\partial r}-\frac{W}{r}\right)^2\right\}$

$\nu_e=\nu+\nu_t$, $\nu_t=C_\mu k^2/\epsilon$

$C_\mu=0.09$, $C_D=1.0$, $C_1=1.44$, $C_2=1.92$, $\sigma_k=1.0$, $\sigma_\epsilon=1.3$

where ϕ, Γ_ϕ, and S_ϕ denote the flow variables, diffusion coefficients and source terms for each variable as given in Table 1.

2.2 Boundary-Fitted Coordinate System

The calculation domain is bounded by the hull surface S, the center-plane C, the water surface W, the upstream section A, the downstream section B, and the outer boundary Σ far from the hull surface as shown Fig. 1. A boundary fittted coordinate is introduced to transform the physical domain in the cylindrical coordinate into a rectangular computational domain in Fig. 2. This transformation can be obtained from the solutions of the following elliptic partial differential equations(Chen and Patel, 1985) :

$$\nabla^2x=0,\quad \nabla^2r=\frac{1}{r},\quad \nabla^2\theta=0 \tag{2}$$

where

$$\nabla^2=g^{11}\frac{\partial^2}{\partial\xi^2}+g^{22}\frac{\partial^2}{\partial\eta^2}+g^{33}\frac{\partial^2}{\partial\zeta^2}+2g^{12}\frac{\partial^2}{\partial\xi\partial\eta}+2g^{13}\frac{\partial^2}{\partial\xi\partial\zeta}+2g^{23}\frac{\partial^2}{\partial\eta\partial\zeta}+f^1\frac{\partial}{\partial\xi}+f^2\frac{\partial}{\partial\eta}+f^3\frac{\partial}{\partial\zeta}$$

, and g^{ij} denote metric tensors, and f^i are control functions for alignment of grid points in the domain.

Design parameters and expermental data are usually presented at each stations of the ship hull. Therefore it is convenient if constant ξ planes are chosen to be coincided with constant x planes. If we put $\xi=\xi(x)$, then following equations are obtained.

$$g^{11}r_{\xi\xi}+g^{22}r_{\eta\eta}+g^{33}r_{\zeta\zeta}+2g^{12}r_{\xi\eta}+2g^{13}r_{\xi\zeta}+2g^{23}r_{\eta\zeta}+f^1r_\xi+f^2r_\eta+f^3r_\zeta=\frac{1}{r} \tag{3}$$

$$g^{11}\theta_{\xi\xi}+g^{22}\theta_{\eta\eta}+g^{33}\theta_{\zeta\zeta}+2g^{12}\theta_{\xi\eta}+2g^{13}\theta_{\xi\zeta}+2g^{23}\theta_{\eta\zeta}+f^1\theta_\xi+f^2\theta_\eta+f^3\theta_\zeta=0 \tag{4}$$

Grid control function f^1 is calculated from the distribution of the x planes. In the radial direction, grid control function f^2 is determined by grid distributions on the inlet and exit plane for grid lines to be smoothlty generated. Grid control function f^3 is prescribed with the grid distribution of the outer boundary.

$$f^1(\xi,\eta,\zeta)=-g^{11}\frac{x_{\xi\xi}}{x_\xi} \tag{5}$$

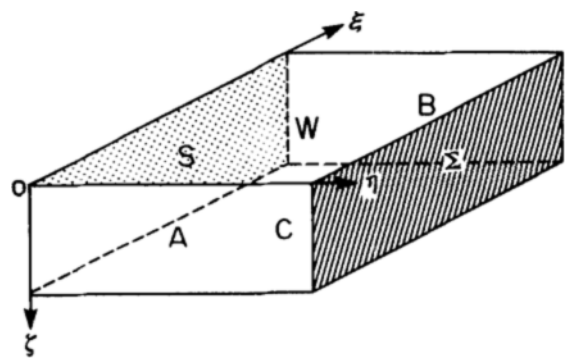

Fig. 2 Computational domain

$$f^2(\xi,\eta,\zeta)=\frac{1}{rr_\eta}+F^2(\xi,\eta,\zeta) \tag{6}$$

$$f^3(\xi,\eta,\zeta)=-g^{33}\left[\frac{\theta_{\zeta\zeta}}{\theta_\zeta}\right]_{\xi=\xi_{in},\eta=\eta_{out}} \tag{7}$$

where

$$F^2(\xi,\eta,\zeta)=\frac{[(\xi_2-\xi)F_1+(\xi-\xi_1)F_2]}{(\xi_{OUT}-\xi_{IN})},$$

$$F_1(\xi,\eta,\zeta)=-g^{22}\left[\frac{r_{\eta\eta}}{r_\eta}\right]_{\xi=\xi_{in}},$$

$$F_2(\xi,\eta,\zeta)=-g^{22}\left[\frac{r_{\eta\eta}}{r_\eta}\right]_{\xi=\xi_{out}}$$

ξ_{IN}, ξ_{OUT} denote values of ξ corresponding to inlet upstream and outlet downstream sections respectively and η_{out} denote the value at the outer boundary. Symmetric Neumann boundary conditions are used at the water plane($\theta=0°$) and the center plane($\theta=90°$). Dirichlet boundary condition is used at other boundaries.

2.3 Transformed Governing Equations

Transformation of independent variables (x, r, θ) in governing equations are considered, leaving velocity components (U, V, W) in the original (x, r, θ) coordinate in Fig. 3. Then governing equations are generally represented as the following form(Oh, 1989).

$$\begin{aligned}&\frac{1}{J}\Big[\frac{\partial}{\partial\xi}(b_1^1U\phi+b_2^1V\phi+b_3^1W\phi)+\frac{\partial}{\partial\eta}(b_1^2U\phi+b_2^2V\phi\\&+b_3^2W\phi)+\frac{\partial}{\partial\zeta}(b_1^3U\phi+b_2^3V\phi+b_3^3W\phi)\Big]\\&=\frac{1}{J}\frac{\partial}{\partial\xi}\Big(\Gamma_\phi Jg^{11}\frac{\partial\phi}{\partial\xi}\Big)+\frac{\partial}{\partial\eta}\Big(\Gamma_\phi Jg^{22}\frac{\partial\phi}{\partial\eta}\Big)\\&+\frac{\partial}{\partial\zeta}\Big(\Gamma_\phi Jg^{33}\frac{\partial\phi}{\partial\zeta}\Big)+S'_\phi\end{aligned} \tag{8}$$

where b_i^j is transformation matrix which can be represented by the partial derivatives of (x,r,θ) with respect to (ξ,η,ζ), and S'_ϕ means the source terms in the transformed equation. Equation(8) can be rendered partially parabolic by neglecting the second order derivative terms with respect to ξ.

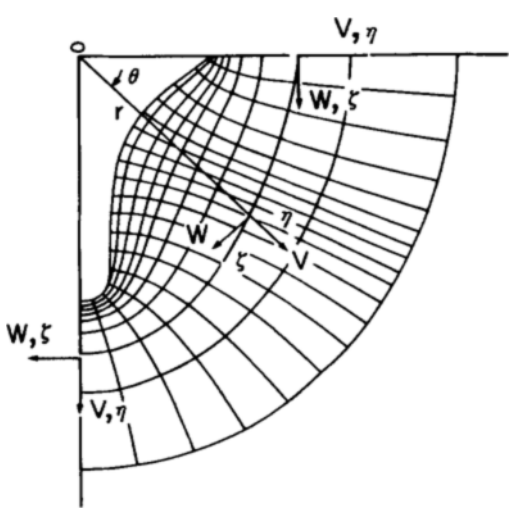

Fig. 3 Body-fitted coordinate system and velocity components

2.4 Boundary Conditions

Boundary conditions at each boundaries of the solution domain are specified as below.

(1) Upstream A ; The position is extended to the upstream as far as thin boundary layer equations and the potential flow theory are valid. The streamwise velocity profile in the boundary layer is specified by 1/7th law

$$\frac{U}{U_e}=\left(\frac{n}{\delta}\right)^{1/7} \tag{9}$$

where n is normal distance from the wall, and δ is boundary layer thickness which is obtained from boundary layer calculation. The velocity in the inviscid region is given as the free stream velocity. The turbulent kinetic energy k and the dissipation rate ϵ are also given by the flat plate coorelations. Pressure is not required by adopting the staggered grid location.

(2) Downstream B ; At one ship length downstream from the stern, zero gradient condition is assumed for the all variables. In the partially parabolic calculation, only the zero pressure gradient condition is required.

(3) Hull surface S ; The grid points next to the wall are located in the fully turbulent layer, and it is assumed the law of the wall is satisfied and the velocity vectors in this region are collateral. The boundary values at the first grid point are given as follows ;

$$\frac{\tau_W}{\rho}=\kappa V_t C_\mu^{1/4}\frac{k^{1/2}}{ln(En_p^+)} \tag{10}$$

$$k=\frac{\tau_W}{\rho C_\mu^{1/2}}, \tag{11}$$

$$\epsilon=\frac{C_\mu^{3/4}k^{3/2}}{\kappa n}, \tag{12}$$

where the velocity at the first grid point near the wall is denoted by V_t and n is nomal distance from the wall, and E is a constant given by 9.793.

(4) External boundary Σ ; It is placed sufficiently far from the hull surface so that uniform flow and no turbulence conditions can be assumed there.

$$U=U_o,\quad W=k=\epsilon=0,\quad p=p_o \tag{13}$$

The radial velocity at the edge of external boundary is determined from the mass conservation.

(5) Center plane C and water plane W ; Symmetric conditions are imposed.

$$W=0,\quad \frac{\partial U}{\partial\zeta}=\frac{\partial V}{\partial\zeta}=\frac{\partial k}{\partial\zeta}=\frac{\partial\epsilon}{\partial\zeta}=0 \tag{14}$$

3. NUMERICAL SCHEME

Grid spacings in the calculation domain are taken as $\Delta\xi=\Delta\eta=\Delta\zeta=1$, and grid control functions are determined by specified values on the boundaries. The grid construction is obtained by solving Eqs.(3),(4) by the finite difference method.

The Finite Volume Method is applied for discretizing the governing equations and the hybrid scheme is employed in the evaluation of the convection terms. The finite difference equations are obtained by integrating the governing equa-

tions over individual control volumes formed by the staggered grids system (Patankar, 1980). Then the final form of the discretized governing equations are obtained as

$$a_P\phi_P = a_N\phi_N + a_S\phi_S + a_E\phi_E + a_W\phi_W + a_U\phi_U + a_D\phi_D + \bar{S}_\phi \quad (15)$$

The subscript P refer to the grid node to be considered and the subscript U,D correspond to the upstream and downstream grid respectively. The other neighbouring grids in the sections are given by the subscript N,S,E,W. If the partially parabolic form of Eq.(8) is integrated, the discretized equations becomes

$$a_P\phi_P = a_N\phi_N + a_S\phi_S + a_E\phi_E + a_W\phi_W + C_u\phi_U + \bar{S}_\phi \quad (16)$$

Since the diffusion term in the ξ direction is removed from the Eq.(8), only the convection term C_u is included in the ξ direction.

The unknown variables(U, V, W, k, ϵ) can be solved by the Eqs.(15),(16) under the known pressures. The pressures are indirectly corrected by SIMPLE(Semi-Implicit Pressure Linked Equation) algorithm (Patankar, 1980), and the discretized equation for the pressure correction is obtained as the same form with the Eq.(15).

$$a_P p'_P = a_N p'_N + a_S p'_S + a_E p'_E + a_W p'_W + a_U p'_U + a_D p'_D + \bar{S}_{P'} \quad (17)$$

In the fully elliptic calculation, the flow variables are iteratively solved after the solutions converge. The procedures are summarized as:

(1) Construct the coordinate system, and calculate the metric tensors and Jacobian.
(2) Specify initial conditions at the inlet plane.
(3) Solve the velocities with assumed or previously calculated pressures.
(4) Solve the pressure-correction equations
(5) Correct pressure distributions and velocities.
(6) Calculate the k,ϵ.
(7) Return to step(3) and repeat step(3) ~ (7) untill the residues are reduced by 0.1% of the reference values.

In the partially parabolic method, pressures of the whole domain are stored by the marching procedure and several sweeps in the ξ-direction are done for obtaining the converged pressures. The procedure are summarized as:

(1) Construct the coordinate system, and calculate the metric tensors and Jacobian.
(2) Specify initial conditions at the upstream boundary.
(3) Calculate velocities at the downstream with the previously calculated pressures.
(4) Correct the pressure distributions and velocities.
(5) Calculate k, ϵ at the downstream
(6) Marching to the downstream boundary.
(7) Return to step(3) and repeat step(3) ~ (6) untill the mass residue is reduced by 0.1% of the reference value.

4. CALCULATIONS AND DISCUSSION

In the present study, two different methods have been intensively investigated and compared by simulating flows over the SSPA 720 model and a multi purpose barge type ship. SSPA 720 model is a container ship model, which was tested in the wind-tunnel by Larsson(1974) and used as one of standard models. The body plan and experimental details are shown in Fig. 4. The latter model has a barge type hull, which was chosen to investigate the possibility of the numerical

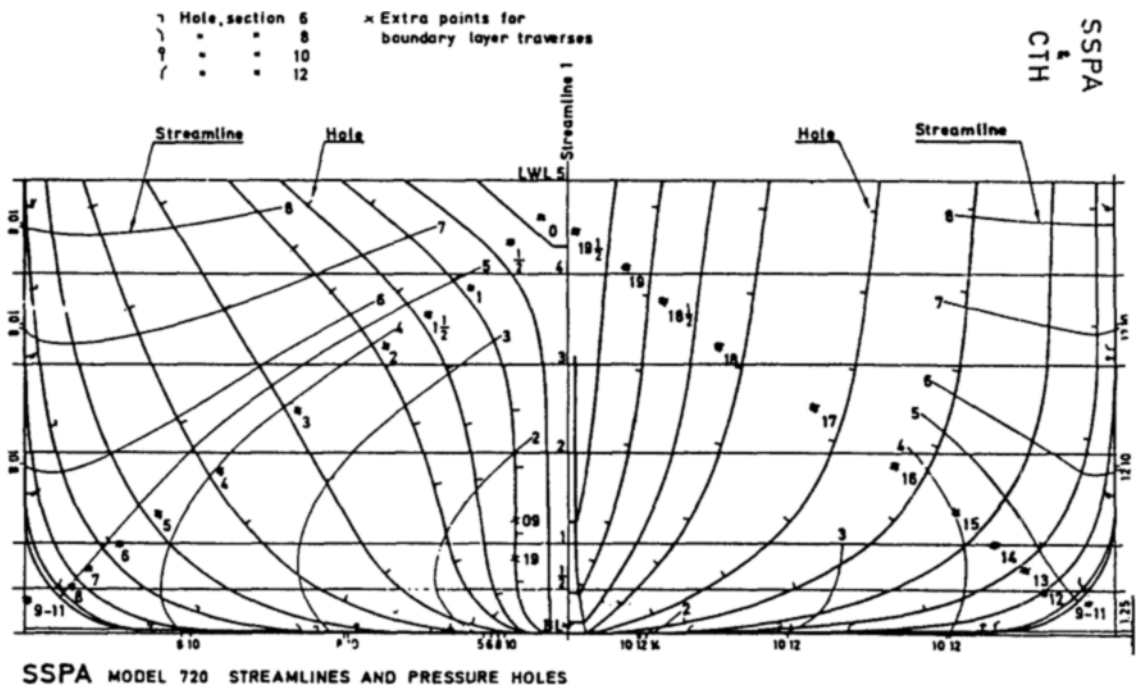

Fig. 4 Body plan of the SSPA model

simulation of viscous flows for ship design purposes.

4.1 SSPA 720 Model

Part of the numerically generated grid system is presented in Fig. 5. Numbers of meshes in the (ξ, η, ζ)-directions are (58,20,14) respectively. They cover the calulation domain of $0.5<x/L<2.0$, $r/L<0.8$. Circumferential grids are distributed to coincide with external streamlines along which measurements have been taken. Along the streamline 1 of the bottom of the hull shown in Fig. 4, the boundary layer becomes very thin from the divergence of streamlines, on the other hand, along the stremline 5 and 7 there makes very thick boundary layer from the convergence of flow streams. Meshes in the radial direction are progressively closely spaced near the hull. Calculation is performed at a Reynolds number, $Re=5.0\times10^6$, where the model was tested in the wind tunnel. Converged solutions are obtained after 90 sweeps by STERN/PPNS and 190 iterations by STERN/NS. The PPNS procedures have internal iterations between upstream and downstream sections and, therefore, the CPU time for one sweep is a little more than for one iteration of the NS procedure. But totally PPNS procedure can save CPU time by 20 percent, as given in Table 2.

Estimated pressure coefficients along each streamlines are shown in Fig. 6. Both calculations are in very good agreement with blockage corrected values(noted by BLCK). However, some attenuations appear in the estimated pressures just over the stern by using fully elliptic calculations. Such attenuations might be originated from neglected longitudinal diffusion terms in the partially parabolic method. It is also confirmed that both method reasonably simulate the interaction between the thick boundary layer and the external inviscid flow. The predicted skin friction coefficients are also qualitatively in good accordance with measurements except some difference near the stern as shown in Fig. 7. The discrepancy near the stern is considered as being due to the inadequacy of standard wall function approach in the region with pressure gradient and wall curvature. It is seen that skin frictions are much reduced over the stern except the streamline 1 of the bottom of the hull where the boundary layer becomes very thin. Girthwise distribution of pressure coefficients and skin friction coefficients are compared with measured values at $x/L=0.9$ in Fig. 8 and Fig. 9. They show sharp gradient near the bottom of the hull because the shear layer rapidly grows thick at the mid-girth and there makes strong interactions from the change of the shear layer.

Distributions of the total velocity at several points, where each streamlines intersect with the $x/L=0.95$ section, are compared with measured data in Fig. 10. Here it should be

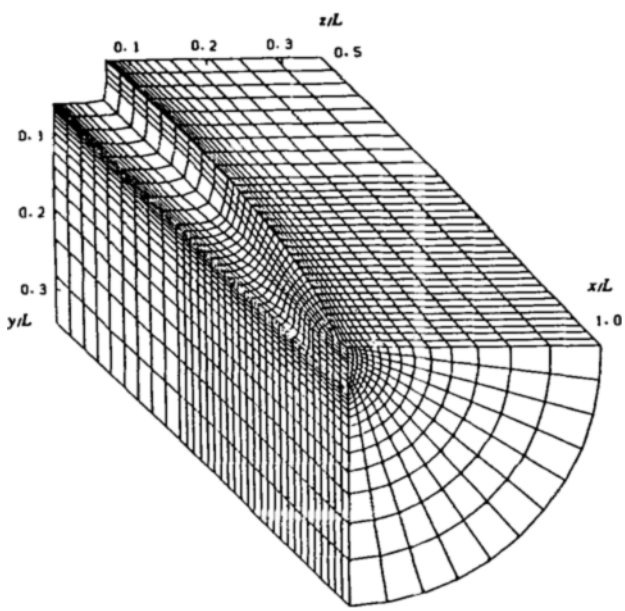

Fig. 5 Over-view of generated grids of SSPA model

Table 2 Calculated models, required sweep(iteration) and CPU time

Model	Total Grid	Numerical Procedure	Sweep (Iteration)	CPU time (SEC)
SSPA-720 Model	53×20×14	PPNS	90	400
		NS	190	500
Barge Type Ship Form	54×25×32	PPNS	90	1300
		NS	190	1600

note: Calculation is made on Fujitz VP-100 supercomputer

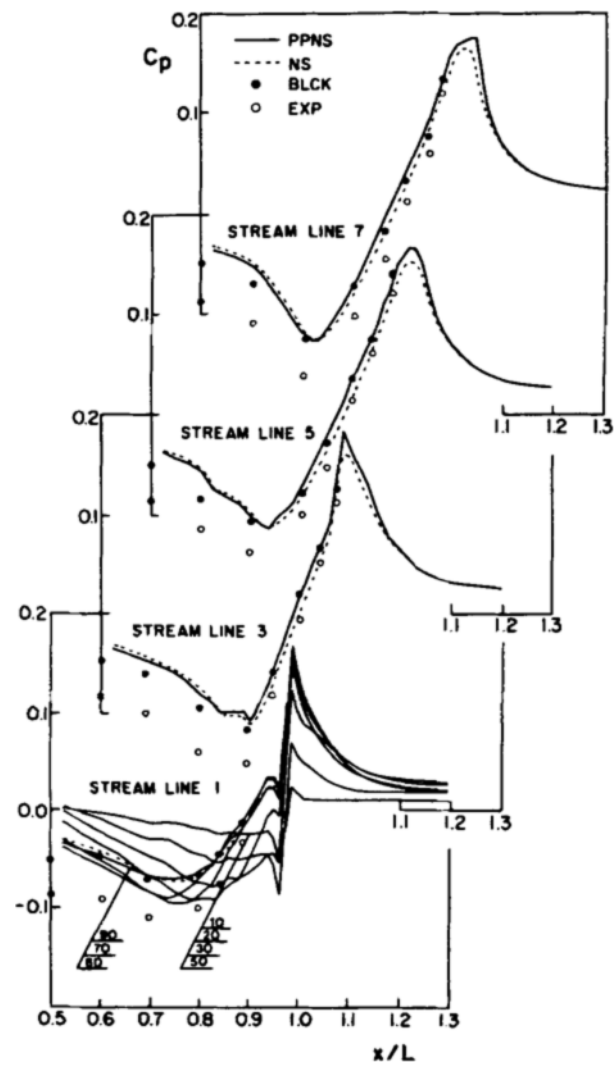

Fig. 6 Pressure distribution over several streamlines on the SSPA model

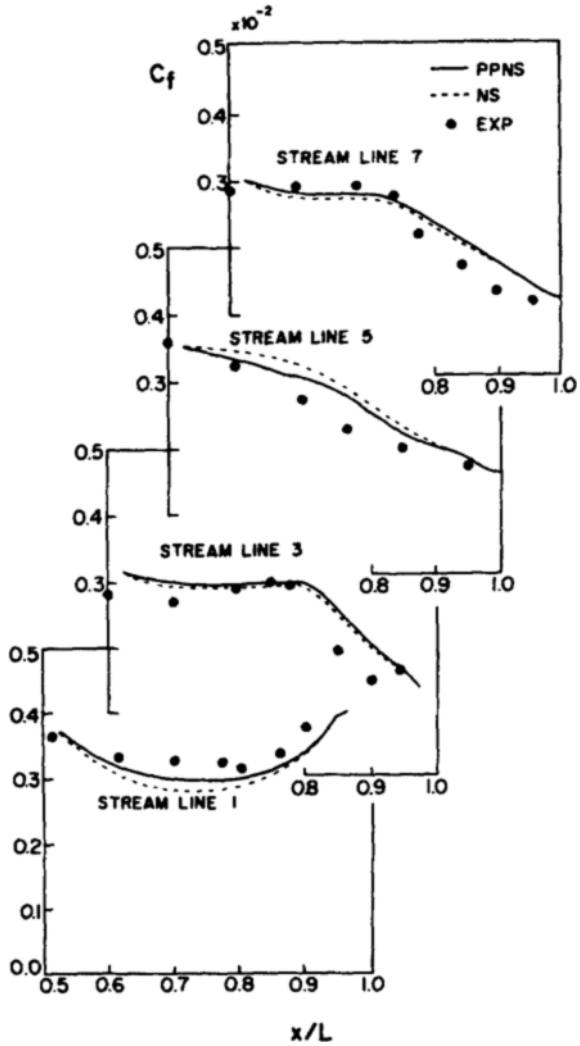

Fig. 7 Skin-friction coefficients distribution over several streamlines on the SSPA model

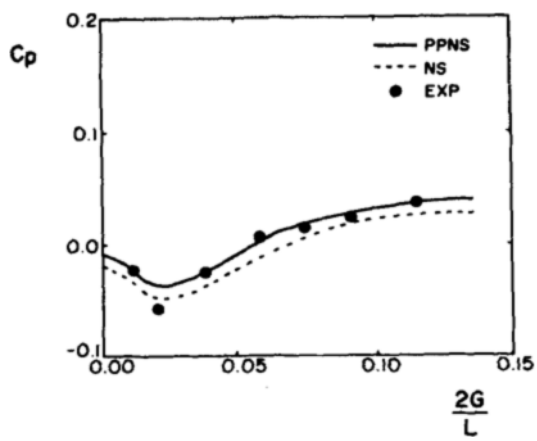

Fig. 8 Girth-wise variation of pressure coefficient at $x/L=0.9$ of the SSPA model (G ; girth-wise length measured from the bottom of hull in the ship section)

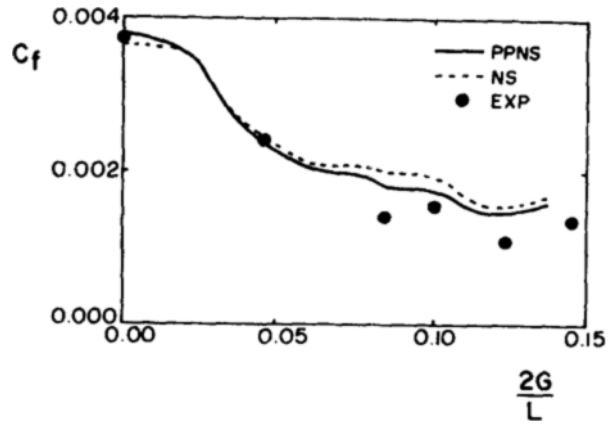

Fig. 9 Girth-wise variation of skin-friction coefficient at $x/L=0.9$ of the SSPA model

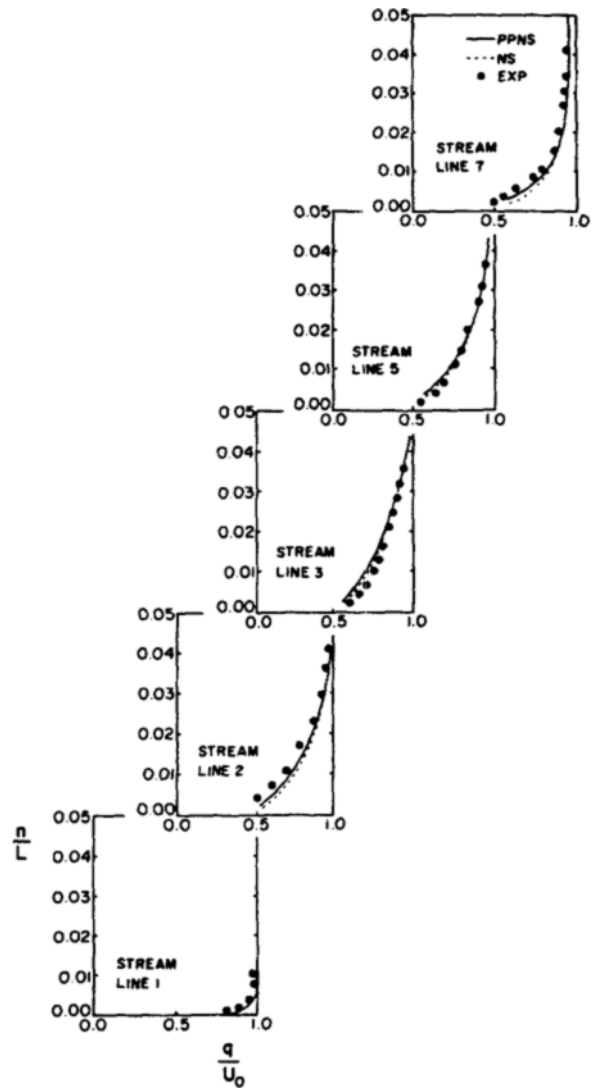

Fig. 10 Profiles of resultant velocity at $x/L=0.95$ of the SSPA model

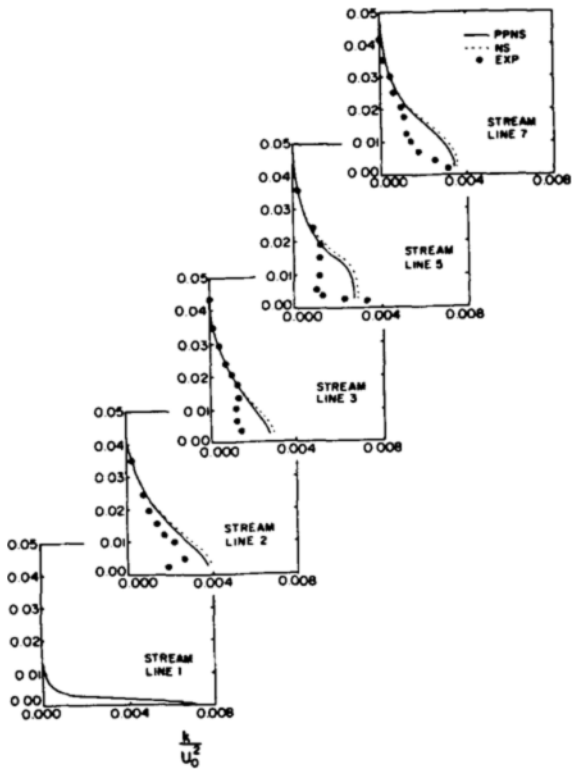

Fig. 11 Profiles of turbulent kinetic energy at $x/L=0.95$ of the SSPA model

noted that measurements are obtained normal to the hull and calculations are computed on transverse sections. There are good agreements between calculations and measurements, although some errors from the difference in the location is involved. Turbulence kinetic energy distributions at $x/L=0.95$ are compared with measured values in Fig. 11. Turbulence kinetic energy shows considerable reduction in the magnitude near the hull over stream line 3,5, and 7, which is quite a unusual feature in the thin boundary layer. This typical characters in the stern flow is due to the strong flow convergence without enough generation of the turbulence kinetic energy over the stern. It is seen that the k-ϵ model adopted in the present calculation fails to capture such a phenomenon over the stern.

4.2 Barge Type Ship

An important object of the present study is to investigate the potentiality of programs for ship design purposes. The selected model, 37K PROBOCON, was originally designed by KSEC(Korea Shipbuilding and Engineering Co.) and developed by SSPA through several series tests in the towing tank. The body plane is shown in Fig. 12. For this model, components of the resistance coefficient and nominal wake distributions are measured in the towing tank at a Reynolds number, $Re=8.5\times10^6$. Furthermore pressure distributions on the corresponsing double body have been measured in the wind tunne(Kang et al., 1987b) although it is carried out at a different Reynolds number, $Re=2.0\times10^6$.

Numerically generated grids are shon in Fig. 13. Numbers of mesh points in the(ξ, η, ζ)-directions are (54,25,23) respectively. Calculation is performed in the domain of $0.5<x/L<2.0$, $r/L<0.963$, and at a towing tank Reynolds number, $Re=8.5\times10^6$. Converged solutions are obtained after 90 sweeps with STERN/PPNS and 190 iterations with STERN/NS. The partially parabolic method can save same amount of CPU time as the previous SSPA-720 model as given in Table 2.

In Fig. 14 pressure coefficient distributions at several station are compared with measured one in the wind-tunnel experiment$(Re=2.0\times10^6)$ and also, potential values by the inviscid calculation. This comparison involves Reynolds number difference and blockage effect in the experiment as can be seen in the comparison at thin boundary layer region of $x/L=0.8,0.85$. The present methods generally show good performance of the pressure estimation on the hull, while the potential flow theory does not properly simulate pressures, especially near $\theta=30°-40°$. It is also indicated that the fully

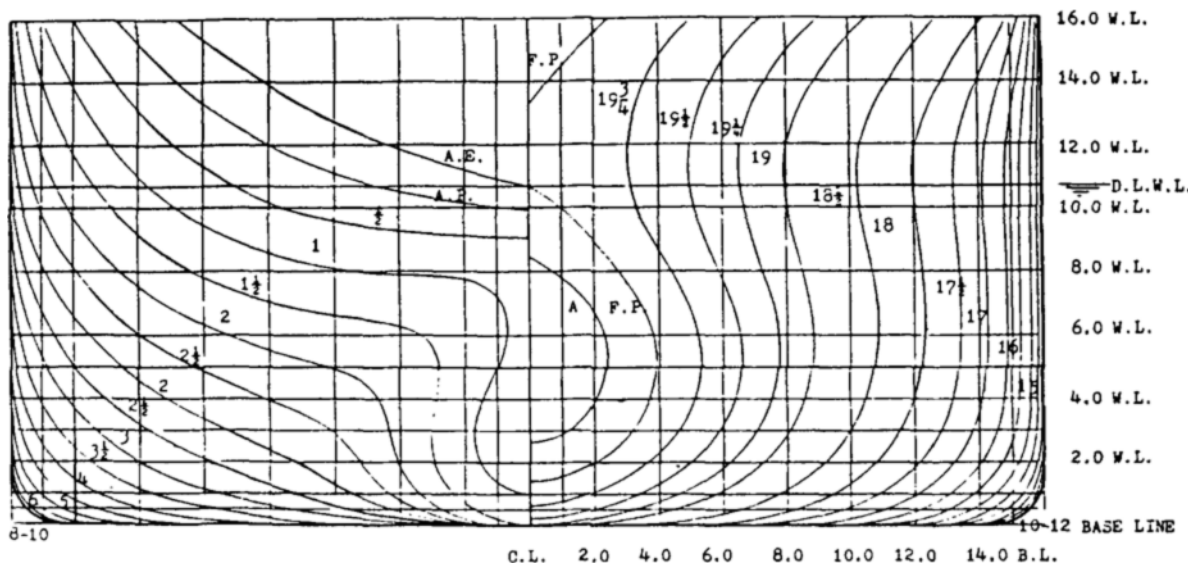

Fig. 12 Body plan of 37K PROBOCON

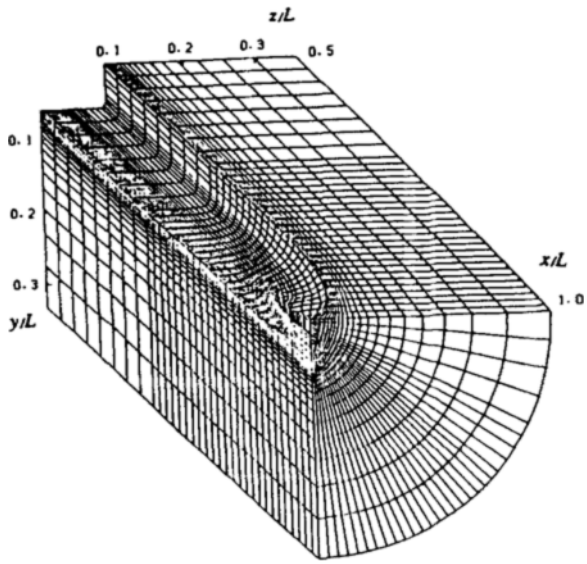

Fig. 13 Over-vew of generated grids of 37K PROBOCON

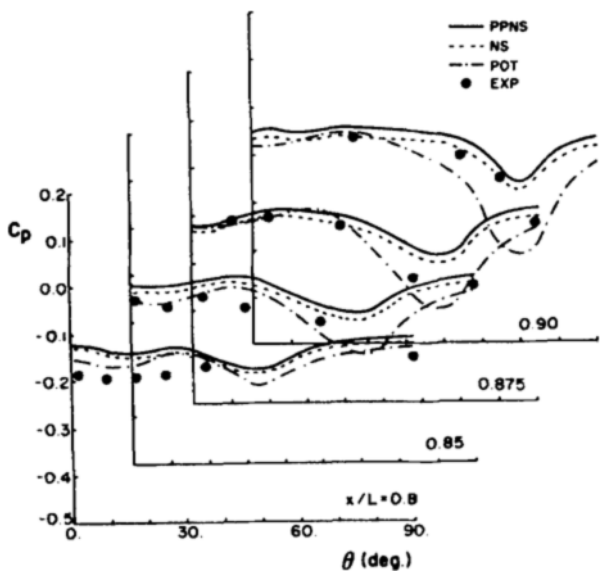

Fig. 14 Girth-wise variatons of pressures at several stations of 37K PROBOCON

elliptic method gives somewhat lower predictions of pressure near the tail of body.

The nominal wakes without propeller in the propeller plane is estimated and compared with measured data in Fig. 15. Wake fractions have been measured at four radial position in the propeller region (0.4R, 0.64R, 0.88R, 1.12R, R; the radius of propeller) and comparison is made at this position. Estimations are generally acceptable at the outer part of propeller plane (1.12R, 0.08R, and 0.64R), but at the innermost part (0.4R), there is much discrepancy between two results. In the present calculation, enough numer of grid cannot be allocated for the local region of propeller plane. And, especilly, it is

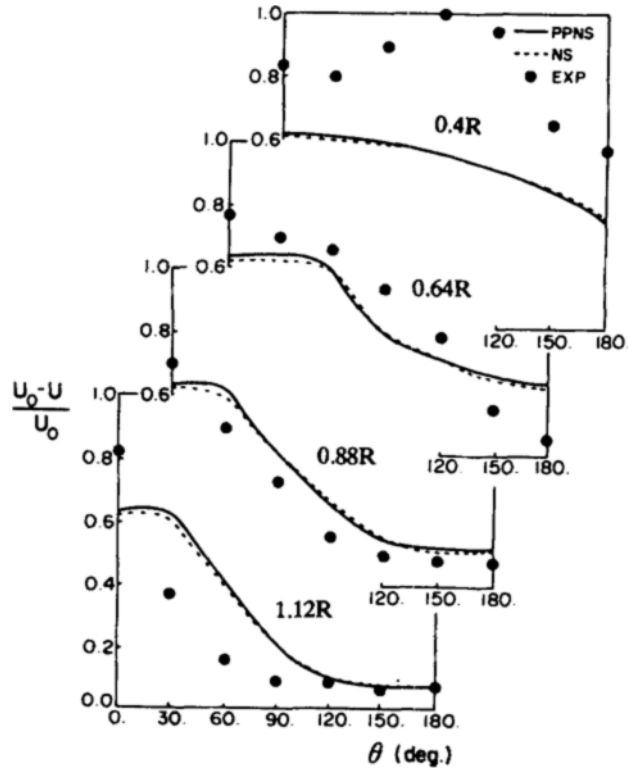

Fig. 15 Variations of wake fraction of 37K PROBOCON in the propeller plane ($x/L=0.975$) without propeller

noted that near the innermost part of the propellar plane between stern bulb and propeller hub only a few mesh points are placed. Hence, calculated result has a little variation along the circumferential direction in comparison with measured data. As far as grid generations are concerned setting aside the validity of the turbulence model and numerical scheme, it should be studied further how to effectively distribute enough number of mesh in the local interest region in the calculation domain.

Finally the capability of codes to estimate the viscous resistance is investigated. The viscous resistance is calculated by a simple wake survey method (Kang and Hyun, 1982) give by

$$C_v = \frac{\rho g \int_{Wa}\left[(H_o - H - \frac{1}{2g}(U_o - (U_o^2 - 2g(H_o - H))^{1/2})^2\right]dS}{\frac{1}{2}\rho U_o^2 S_w} \quad (18)$$

where $H_o = p_o + \rho U_o^2/2$, $H = p + \rho U^2/2$ and S_w is the wetted surface area of the hull. The integration position of the wake (Wa) is half the ship-length downstrean from the stern. Estimated coefficients of the viscous resistance by the partially parabolic method and by the fully elliptic method are 3.57×10^{-3} and 3.62×10^{-3} respectively. In view of the measured values 3.9×10^{-3}, all the simulation errors, i.e. presures and velocities, are summed up to show 10% under-estimation. If we take into account such uncertainties, the present predictions are considered acceptable, and the computer codes may be useful for the hull form design.

5. CONCLUSION

(1) Two simulated results by the partially parabolic and fully elliptic Navier-Stokes equations are shown to be nearly identical. This indicated that the effects of streamwise dffusion terms are negligible when the flow reversal does not appear over the stern. The partially parabolic method requires only half of the memory storage and saves CPU time by 20% in comparison with the fully elliptic method.

(2) The standard form of k-ϵ model usually over-predicts the turbulent kinetic energy and cannot properly account for the reduction of the turbulent kinetic energy near the wall when the viscous layer becomes thick over the stern.

(3) Simulated nominal wake fractions show acceptable agreement with wake measurements except the inner-most part of the propeller region. For more accurate prediction, it should be studied further how to allocate enough number of meshes locally over the propeller plane, as well as globally over each ship sections.

(4) A coefficients of the viscous resistance predicted by the present method are shown to be under-estimated by 10 percent and the present method can provide useful estimation of viscous resistance for the hull form design.

REFERENCES

Abdelmeguid, A.M., Markatos, N.C., Muraoka, K. and Spalding, D. B., 1979, "A Comparison Between the Parabolic and Partially Parabolic Solution Procedures for Three-Dimensional Turbulant Flows around Ship's Hull," Appl. Math. Modelling, Vol. 3, pp. 525~538.

Chen, H.C. and Patel, V.C., 1985, "Calculation of Trailing-Edge, Stern and Wake Flows by a Time Marching Solution of the Partially-Parabolic Equations," IIHR Report No. 285, Iowa Inst. Hydraulic Research, University of Iowa.

Janson, C.E. and Larsson, L., 1985, "Ship Flow Calculations Using the PHOENICS Computer Code, Proc. 2nd Int. Symp. on Ship Viscous Resistence," Sweden, p. 17 :1.

Kang, S. and Hyun, B., 1982, " A Simple Estimation of the Viscous Resistance of Ships by Wake Survey," J. Soc. Naval Arch. of Korea, Vol. 19, No. 2, pp. 19~25.

Kang, S., Oh K. and Lee S., 1987, Study on the Stern Design by Using the Viscous Flow Simulation, RIIS Report 87-092, Research Inst. Industrial Science, Seoul Nat. University.

Kang, S., Yoo, J., Shon, B., Lee S. and Baik, S., 1987, "Experimental Study on Viscous Flows around Ship Sterns by Using the Hot-Wire Anemometer in the Wind-Tunnel, J. Soc. Naval Arch of Korea, Vol. 25, No. 3, pp. 13~18.

Kang, S. and Oh, K., 1988, "Numerical Calculation of Three Dimensional Viscous Flow over a Barge type Stern by Semi-Elliptic Equation, Seminar on Ship Hydrodynamics, Seoul, pp. 32~39.

Kang, S. and Oh, K., 1987, "Numerical Calculations of Three-Dimensional Viscous Stern-Flows by Semi-Elliptic Equations," J. Soc. Naval Arch. of Korea, Vol. 26, No. 1, pp. 11~23.

Larsson, L., 1974, Boundary Layers of Ships. Part 3 : An Experimental Investigation of the Turbulent Boundary Layer on a Ship Model, SSPA Report No. 46, SSPA, Sweden.

Larsson, L., 1981, "SSPA-ITTC Workshop on Boundary Layers-Proceedings," SSPA-Publication No. 90, SSPA, Sweden.

Muraoka, K., 1980, "Calculation of Thick Boundary Layer and Wake of Ships by a Partially Parabolic Method," Proc. 13th ONR Symp., Tokyo, pp. 601~616.

Muraoka, K., 1982, "Calculation of Viscous Flow around Ships with Parabolic and Partially Parabolic Solution Procedures, Trans. West Japen Soc. Naval Arch., Vol. 63, pp. 13~29.

Oh, K., 1989, Numerical Study on the Viscous Flows over the Ship Stern, Ph. D. Thesis, Dept. of Mech. Eng., Seoul Nat. University.

Patankar, S.V., 1980, Numerical Heat Transfer and Fluid Flow, McGraw-Hill, New York.

Patel, V.C., 1982, "Some Aspects of Thick Three-Dimensional Boundary Layers," Proc. 14th ONR Symp., Ann Arbour, pp. 999~1040.

Pratap, V.S. and Spalding, D.B., 1976, "Fluid Flow and Heat Transfer in Three-Dimensional Duct Flows," Int. Journal of Heat and Mass Transfer, Vol. 19, pp. 1183~1188.

Raven, H.C. and Hoekstra, M., 1985, "A Parabolized Navier-Stokes Solution Method for Ship Stern Flow Calculations," 2nd Int. Symp. on Ship Viscous Resistence, Sweden, p. 14 : 1.

SSPA, 1987, 37K PROBOCON Wake Measurements, Report 3202-12, Sweden.

Tzabiras, G.D., 1985, "On the Calculation of the 3-D Reynolds Stress Tensor by Two Algorithm," 2nd Int. Symp. on Ship Viscous Resistence, Sweden, p. 15 : 1.